ARTICLES

Dynamical Time Scales of Aqueous Solvation at Negatively Charged Lipid/Water Interfaces†

Alexander V. Benderskii and Kenneth B. Eisenthal*

Department of Chemistry, Columbia University, New York, New York 10027

Received: May 24, 2001; In Final Form: August 23, 2001

Time-resolved second harmonic generation spectroscopy of a solvatochromic dye coumarin 314 was used to investigate how the solvation dynamics at the air/water interface are affected by lipid surfactants with anionic carboxylate and sulfate headgroups. The surfactants were chosen to mimic common functional groups and the negative charge of biological aqueous interfaces such as cell membranes and folded proteins. The diffusive component of the solvation response, associated with rearrangement of the water hydrogen bond network, exhibits a biexponential decay. The two time scales change as a function of the surface charge density, compared to the bare air/water interface solvation dynamics, $\tau_1 = 250 \pm 50$ fs and $\tau_2 = 2.0 \pm 0.4$ ps, which are similar to the bulk water response, $\tau_1 = 130-250$ fs and $\tau_2 = 0.6-1.2$ ps. The faster τ_1 component is unaffected at low to intermediate sulfate surface coverage (270 ± 50 fs at 500 Å^2/molecule and 225 ± 25 fs at 250 Å^2/molecule) but becomes slower at high surface coverage (100 Å^2/molecule), 600 ± 70 fs. The slower τ_2 component changes even at the lowest coverage: $\tau_2 = 4.4 \pm 0.9$ ps at 500 Å^2/molecule; 5.2 ± 0.7 ps at 250 Å^2/molecule; and 5.4 ± 1.1 ps at 100 Å^2/molecule. Different behavior of the two solvation components indicates that they represent different water motions. The solvation dynamics compared with the structure-sensitive surface vibrational spectroscopy of the same interface [Gragson, D. E.; McCarty, B. M.; Richmond, G. L. *J. Am. Chem. Soc.* **1997**, *119*, 6144. Gragson, D. E.; Richmond, G. L. *J. Am. Chem. Soc.* **1998**, *120*, 366.] show a similar dependence on surfactant coverage. For the first time, to our knowledge, a relation is made between a dynamical relaxation mode, the slower diffusive solvation time scale τ_2, and a spectral feature, in this case the strongly hydrogen-bonded water structures induced by the negative surface charge. The carboxylate and sulfate surfactants induce similar dynamics, suggesting that the solvation is not sensitive to the chemical composition of the headgroup but rather to the total negative surface charge density.

Introduction

Many of the naturally occurring aqueous interfaces are charged. On a very general level, this is a manifestation of the asymmetry of interfaces: many species dissociate in the presence of water, and the positive and negative ions often exhibit a different tendency to stay at the surface (e.g., because of adsorption or chemical bonding) vs solubility in the bulk. Several particularly important examples of charged aqueous interfaces are found in biology: cell membranes are negatively charged because of the presence of anionic phospholipids in the lipid bilayer; folded proteins expose hydrophilic functional groups, which are often ionic, to the water phase. These interfaces host a variety of vital reactions involved in protein interactions, enzyme catalysis, molecular recognition, and various steps of the electron transfer pathways. Properties of water as a solvent near these charged surfaces are extremely important in determining how adsorption, desorption, and chemical reactions will proceed in these special restricted environments. Solvation structures of water near an interface determine free energies of the interfacial species, their adsorption, and chemical equilibria, whereas dynamical characteristics such as solvation response times influence the rates of surface reactions.[1]

A simplified model system was used in this study to mimic negatively charged biointerfaces. The air/water interface is covered with a monolayer of an amphiphilic lipid surfactant with an anionic (carboxyl or sulfate) headgroup. This way we can study how equilibrium and dynamical properties of water near the interface are changed due to a single (anionic) functional group instead of a multitude of hydrophilic functionalities composing a typical biointerface. Variation of the surfactant density allows the study of how the solvent properties change as a function of the surface charge, whereas comparison of different surfactants at similar surface densities isolates the effect of the chemical composition of the hydrophilic headgroups.

Our measurements primarily focused on the solvation dynamics of water near the negatively charged lipid interfaces. Solvation dynamics characterize the response of the solvent to a sudden change in the charge distribution of an adsorbed solute molecule. It was monitored via the femtosecond time-resolved second harmonic generation (TRSHG) spectroscopy of a solvatochromic probe molecule coumarin 314 (C314). This method

† Part of the special issue "G. Wilse Robinson Festschrift".

* To whom correspondence should be addressed.

10.1021/jp0120155 CCC: $22.00
Published on Web 11/17/2001

combines ultrafast time resolution with surface selectivity, so that only the molecules adsorbed at the interface are detected.

It was recognized a long time ago that the dynamical time scales of solvent reorganization have a profound influence on the rates and mechanisms of redox reactions.[2] Further theoretical developments demonstrated that solvation dynamics often determine the rate of the elementary electron-transfer step.[3] Extensive experimental and theoretical efforts were undertaken to measure and understand the ultrafast solvation response of bulk polar solvents,[4] in particular water.[5] The bulk-phase aqueous solvation is characterized by three temporal components. The so-called inertial component has a Gaussian time dependence of $\tau_i \sim 25$ fs duration and is thought to be due to librational motions of water molecules.[6,7] This is followed by two exponential components which have been termed diffusive: reported values for τ_1 vary from 130 to 250 fs and for τ_2 from 690 to 1200 fs.[4,8] These diffusive components have been assigned to aqueous dynamics involving rearrangement of the hydrogen bond network, i.e., breaking and making water−water H bonds,[6,7] for which similar time scales have been measured using time-resolved vibrational spectroscopy of OH stretch in bulk water.[9,10] Although the temporal resolution of our experiment does not allow observation of the ultrafast inertial component, we report measurements of the two diffusive components of aqueous solvation at negatively charged lipid interfaces. We report how these time scales associated with the dynamics of hydrogen bond rearrangement are changed as a function of the surfactant coverage, i.e., the surface charge density.

The following simple estimate shows that it is to be expected that the structure of water, e.g., the average orientation of water dipoles, is significantly altered in the vicinity of a charged interface. The surface charge density of a typical biointerface may range from 5 to 30 μC/cm^2, corresponding to 50−300 Å^2 per charged group,[11] resulting in the interfacial electric field of the order of $0.5-3 \times 10^8$ V/m. The interaction energy of a water dipole ($\mu_{H_2O} = 1.85$ D) with this field may be up to 0.5 k_BT. The alignment of water molecules near the interface may lead to hydrogen-bond patterns that are different from the randomly oriented hydrogen bond patterns of bulk phase water. This, in turn, would imply that the dynamical behavior of the interfacial water, in particular the diffusive solvation time scales, should differ from the bulk-phase response times. Structural changes of water near a charged interface have been observed by several experimental techniques, including surface-enhanced FTIR,[12,13] sum−frequency generation (SFG),[14,15] and X-ray scattering of charged metal electrodes.[16] Particularly relevant to the present case is the vibrational SFG study of the OH stretch of water at the air/water interface covered with a sodium dodecyl sulfate surfactant, where both static alignment of water molecules and increased hydrogen bonding were observed.[14,15] Our measurements of the dynamics of water at the same interface may help elucidate the structure−dynamics relationship of this important aqueous environment.

The observed effects of the electrostatic field on water properties should be applicable to any type of charged aqueous interface. Indeed, our experiments indicate that similar aqueous solvation dynamics are induced by the *negatively charged* lipids of different chemical composition, C_{12} sulfate and C_{17} carboxylate; that is, the solvation dynamics seem to be sensitive only to the total negative charge of the interface. On the contrary, for the *neutral* C_{17} carboxyl surfactant (stearic acid) at the air/water interface, a very different solvation response was discovered as reported previously:[17] only the faster ($\tau_1 = 400$ fs) component of the diffusive was observed, whereas the slower τ_2 component was suppressed. This may be attributed to local interactions such as hydrogen bonding of neutral hydrophilic headgroups with water molecules that are specific to each surface moiety.

In a preliminary report, solvation dynamics at the negatively charged stearic acid (C_{17}) surfactant air/water interface[18] were found to proceed slower than at the neutral stearic acid monolayer[17] and slower than at the surfactant-free air/water interface.[17,19] However, only the overall solvation response time scale for the carboxylate monolayer $\tau_S = 1.6 \pm 0.3$ ps was reported. Here, we describe measurements at carboxylate and sulfate anionic monolayers, as a function of the surfactant density with an improved signal-to-noise ratio which allows clear observation of the two diffusive solvation dynamics components τ_1 and τ_2. Both time scales increase at the negatively charged interface. However, we discover that the two components show different dependence on the anionic surfactant coverage, indicating that they represent different water motions. In the Discussion section, our results are compared with the available data on the ultrafast solvation dynamics in bulk water,[4,5,8] in protein and DNA hydration shells,[20] in restricted environments such as reverse micelles,[21] and with recent measurements of the H-bond dynamics in the hydration shells of anions.[22]

Experimental Section

The probe laser beam is incident at 70° from vertical onto the air/water interface of the sample solution contained in a shallow Teflon beaker. The reflected beam contains a weak second harmonic (2ω) signal generated at the interface. The 2ω signal is filtered from the fundamental frequency (ω) light using two blue (short-pass) filters and a Jarrel Ash monochromator and registered by a photomultiplier (Hamamatsu. model R4220P). The sample solutions contained 15 μM of coumarin 314 (Acros, laser grade) which adsorbs to the surface and gives a strong resonantly enhanced second harmonic signal. Doubly distilled water was used to prepare all solutions, and the sample beakers were cleaned using the piranha solution (1:2 H_2O_2: concentrated H_2SO_4) prior to each measurement to avoid organic contaminants on the surface.

The pump−probe TRSHG setup is based on a regeneratively amplified Ti:sapphire laser system (Clark-MXR) which operates at 1 kHz and produces 120 fs pulses. The fundamental wavelength is used for the probe beam, $\lambda_{pr} = 840$ nm (45 μJ/pulse), whereas a small portion of the output is frequency-doubled in a BBO crystal to produce the pump beam $\lambda_{pu} = 420$ nm (1 μJ/pulse). Details of the pump−probe setup are described elsewhere.[17,18] The pump and probe beams are overlapped at the sample surface at a 5° horizontal separation angle. The spot size of the pump beam is ∼0.5 mm, corresponding to the average power density of ∼300 mW/cm^2 in the pump beam. We note that the probe beam is not one-photon resonant with the C314 dye molecules. The sample beaker is placed on a rotary stage operating at 4 rpm, and the pump and probe laser beam spots are 1.0−1.5 cm off center. This minimizes local heating, desorption, and bleaching of the C314 dye by the one-photon resonant pump beam.

When sodium dodecyl sulfate (SDS), $CH_3(CH_2)_{11}OSO_3^-\ Na^+$, a water-soluble surfactant, is added to the sample solution, the amphiphilic dodecyl sulfate adsorbs to the air/water interface forming a negatively charged molecular layer, whereas the sodium cations remain in solution. The surface density Γ_{SDS} of the anionic lipid at submonolayer to monolayer coverage is

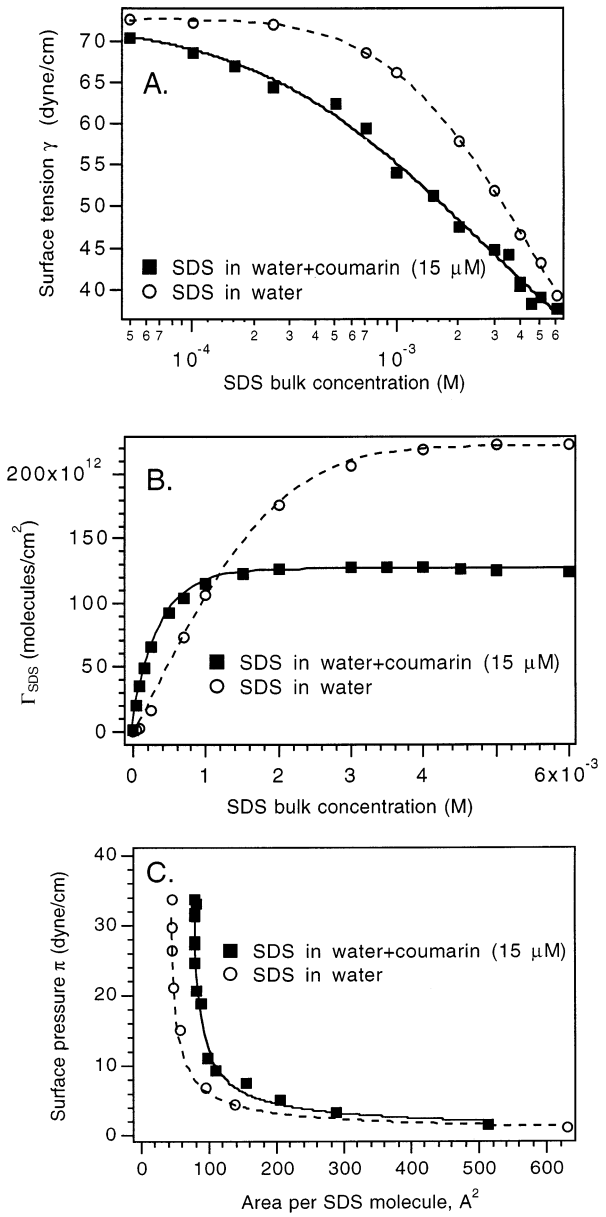

Figure 1. (A) Surface tension of SDS solutions in water (○) and in 15 μM coumarin 314 water solution (■) as a function of SDS bulk concentration. (B) Calculated surface density of SDS as a function of SDS bulk concentration. (C) 2D phase diagram (surface pressure π vs area per SDS molecule) of SDS Gibbs monolayers on water (○) and on a 15 μM coumarin 314 water solution (■).

determined by the bulk SDS concentration C_{SDS}, as described by the Gibbs adsorption isotherm

$$\Gamma_{SDS} = -\frac{1}{2RT}\frac{\partial\gamma}{\partial[\ln C_{SDS}]} \qquad (1)$$

where the factor 2 in the denominator reflects adsorption of a completely dissociated ionic surfactant. SDS is often referred to as an ideal surfactant because it obeys eq 1 nearly perfectly.[23] Using a standard Wilhelmy plate setup, the surface tension γ of water-SDS and water-C314−SDS solutions were measured as a function of SDS concentration and the results were fitted to the Gibbs eq 1 to calculate the surface excess of SDS, Γ_{SDS}, as shown in Figure 1. The results for the water−SDS solutions are in good agreement with the literature values.[23] Because C314 is surface active, its presence affects adsorption of SDS, as demonstrated in Figure 1. In particular, the SDS surface

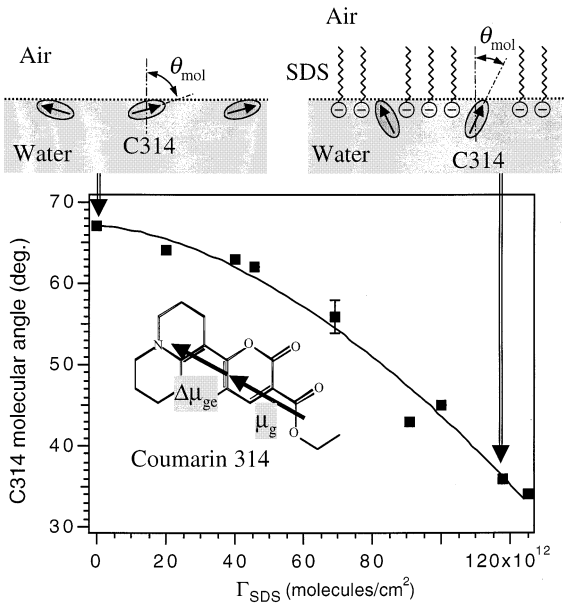

Figure 2. Molecular orientation of coumarin 314 at the air/water interface covered with SDS, as a function of the SDS surface density.

coverage corresponding to a saturated monolayer is ~80 Å²/SDS molecule for the 15 μM C314 solution, whereas in the absence of coumarin, it is ~48 Å²/SDS molecule.[23] This behavior is expected because of the C314 molecules occupying some of the surface, thereby reducing the surface available to SDS molecules. Similar effects were observed for other pairs of surfactants.[17,18,24] Three SDS concentrations, 0.05, 0.125, and 0.6 mM, corresponding to the surface coverage of 500, 250, and 100 Å²/SDS molecule, were chosen for the time-resolved solvation dynamics measurements. Note that all three concentrations are well below the critical micelle concentration (cmc) for SDS, 8 mM.

The carboxylate surfactant used in this study is ionized stearic acid, $CH_3(CH_2)_{16}COO^-$. Preparation of the monolayers of this insoluble surfactant was accomplished by spreading its solution in hexane on the surface of the water−C314 solution using a microsyringe, as described previously.[17,18] The water sub-phase pH was adjusted to 10.5 by adding NaOH to ensure that the stearic acid ($pK_a \approx 5.0$) is completely ionized. The 2D phase diagram of this insoluble surfactant limits its use to a narrow range of surface coverage, ~200 Å²/molecule, where the film is in the uniform liquid phase.[18] A lower coverage would be in the 2D gas−liquid coexistence region, where the film is not uniform and consists of islands of liquid-phase density separated by a very low density "gas" phase, whereas at higher coverage, formation of a second layer and clusters of the surfactant molecules on the surface may occur.

As observed previously, formation of both the sulfate and carboxylate surfactant monolayers at a density of ~200 Å²/molecule reduces the number of adsorbed C314 molecules by approximately a factor of 2 relative to the bare air/water interface.[17,18] Surface concentration of the adsorbed C314 was $\sim 10^{13}$ cm^{-2}, obtained from surface tension measurements of the C314 solutions.[17]

Results

Average molecular orientation of the C314 probe molecules at the SDS air/water interface was measured using the SHG null angle technique,[25] Figure 2, assuming a narrow distribution of orientations. Because our SH probe is in resonance with the $S_1 \leftarrow S_0$ transition of C314, it measures the angle θ_{mol} of the

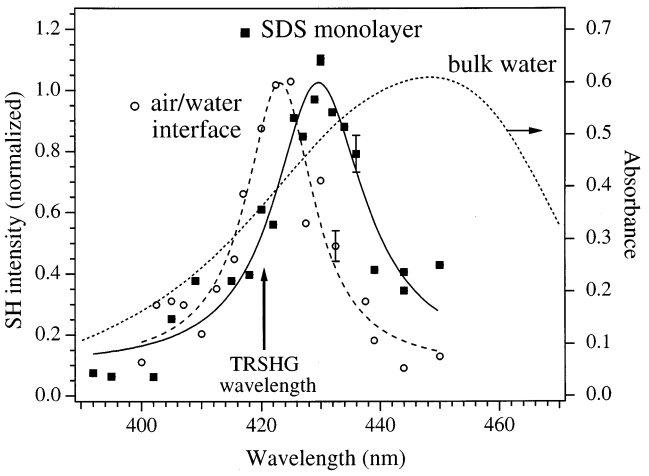

Figure 3. (■) SHG spectra of C314 at the SDS air/water interface (100 Å^2/SDS molecule); (○) same at the surfactant-free air/water interface. Dashed line shows the linear absorption spectrum of C314 in water.

transition dipole moment μ_{ge} with respect to the surface normal, showing that the C314 molecules tend to be more perpendicular to the interface as the SDS surface density increases. In C314, the $S_1 \leftarrow S_0$ *transition* dipole moment of C314 is parallel to its *permanent* dipole moment in the ground state ($\mu_g = 8.2$ D).[26] The results in Figure 2 therefore indicate that the dipolar C314 molecules are aligned by the electrostatic field of the charged interface. Similar results were obtained previously for the negatively charged carboxylate monolayer interface.[18]

The second harmonic spectrum of C314 adsorbed at the SDS air/water interface was recorded as described elsewhere.[17,18] Coumarin 314 is a well-characterized solvatochromic probe,[27] so that its transition frequency (determined by the equilibrium solvation energy) can be used to characterize the polarity at this interface.[28] The SDS bulk concentration was 0.6 mM, corresponding to the Gibbs surface excess $\Gamma_{SDS} = 1 \times 10^{14}$ cm^{-2}, i.e., 100 Å^2/SDS molecule. The peak in the SH spectrum (Figure 3) corresponds to the resonance of the second harmonic probe frequency 2ω with the $S_1 \leftarrow S_0$ transition. The transition frequency at the interface was extracted by fitting the SH spectrum as described in ref 18, $\omega_{ge} = 429 \pm 2$ nm. For comparison, the SH spectrum at the neat air/water interface yields 423 nm, and the linear absorption spectrum of C314 in bulk water peaks at 448 nm. Figure 3 thus shows that the polarity of the SDS interface is intermediate between the surfactant-free air/water interface and bulk water. On the ET(30) polarity scale, the bulk water is 63, the neat air/water interface is 31, and SDS air/water interface is 35. We note that the electrochromic shift of the C314 transition dipole $\mu_{ge} \approx 4$ D in the interfacial field $E \approx 1.3 \times 10^8$ V/m is expected to be of the order of 2 nm, which is within our experimental uncertainty. Although they provide a reliable measure of the equilibrium solvation energies, static electronic spectra carry relatively little information regarding other molecular properties of these interfaces. For example, SH spectrum at the anionic SDS interface, where $\omega_{ge} = 429 \pm 2$ nm, is very similar to that at the neutral stearic acid interface at 200 Å^2/C$_{17}$ molecule, where $\omega_{ge} = 431 \pm 2$ nm.[17] Time-resolved experiments described below show that significant differences exist between the dynamical response of the neutral and charged interfaces.

Femtosecond pump-second harmonic probe spectroscopy of the solvatochromic C314 probe molecules adsorbed at the interface was used to measure the aqueous solvation dynamics. Quantitative details of the time-resolved second harmonic generation (TRSHG) as a probe of the solvation dynamics were presented elsewhere (see, e.g., ref 18). Qualitatively, one-photon resonant pump pulse ($\lambda_{pu} = 420$ nm) excites a small fraction (~5%) of the C314 molecules at the interface to the S_1 electronic state, whose dipole moment ($\mu_e = 12$ D) is larger than that of the ground electronic state S_0 ($\mu_g = 8.2$ D). Relaxation of the solvation environment around the excited molecules is monitored by a time-delayed SH probe pulse. Prior to the excitation, the equilibrium arrangement of polar solvent molecules around the ground-state solute is determined by the solute−solvent interaction energy (primarily dipole−dipole), which tends to partially orient the surrounding solvent molecules along the dipole field lines. The minimum free energy solvent structure around the S_1 excited state C314 will be different because of its larger dipole moment. The temporal evolution of the many-dimensional solvent configuration is usually characterized by projecting it onto a one-dimensional coordinate representing the solvent−solute interaction energy.[8] Its temporal evolution (after a sudden $S_1 \leftarrow S_0$ excitation) is quantified by the solvation correlation function $S(t)$, defined as

$$S(t) = \frac{\omega_{eg}(t) - \omega_{eg}(\infty)}{\omega_{eg}(0) - \omega_{eg}(\infty)} \tag{2}$$

where $\omega_{eg}(t) = (E_e - E_g)/\hbar$ represents the evolving energy gap (i.e., transition frequency) between the excited S_1 and ground S_0 state of the solvated C314. $S(t)$ ranges from 1 for the ground-state configuration at $t = 0$, i.e., immediately after the pump pulse, to 0 for the equilibrium excited-state configuration achieved at $t \rightarrow \infty$.

The SH probe signal is a coherent superposition of the *time-independent* resonant contribution from the ground-state molecules and the *time-dependent* contribution from excited molecules

$$I_{SH}(t) = |\chi^{(2)}|^2 I_{pr}{}^2 \tag{3}$$

where the total second-order surface nonlinear susceptibility is[18,19]

$$\chi^{(2)}(t) = n_g \frac{A_{ge}}{\omega_{ge} - 2\omega + i\Gamma_{ge}} + n_e \frac{A_{eg}}{\omega_{eg}(t) - 2\omega + i\Gamma_{eg}} + B \tag{4}$$

The first term is the *time-independent* ground-state resonant contribution, where n_g represent the ground-state population, ω_{ge} is the ground-to-excited-state $S_1 \leftarrow S_0$ transition frequency, 2ω is the SH probe frequency, Γ_{ge} is the transition width, and A_{ge} contains the transition matrix elements and other terms which are not strongly dependent on frequency. The second term describes the resonant contribution from the excited-state population n_e, where the only *time-dependent* term is the excited-to-ground-state $S_1 \rightarrow S_0$ transition frequency $\omega_{eg}(t)$. The third term B represents a constant nonresonant contribution. At $t = 0$, $\omega_{eg}(0) = \omega_{ge}$, and a decrease in the SH probe signal is observed owing to cancellation of the ground and excited-state contributions, because $A'_{eg} = -A'_{ge}$; for a two state system, the phases of the ground and excited states are of opposite sign.[19,29] Subsequently, solvation lowers the excited-state energy thus red-shifting $\omega_{eg}(t)$. This decreases overlap with the SH probe $\lambda_{pr} = 420$ nm, which in these experiments is on the blue shoulder of the C314 surface spectrum (Figure 3), i.e., shifts the excited state out of the resonance, and results in a partial recovery of the SH signal intensity as a function of the pump−probe delay.

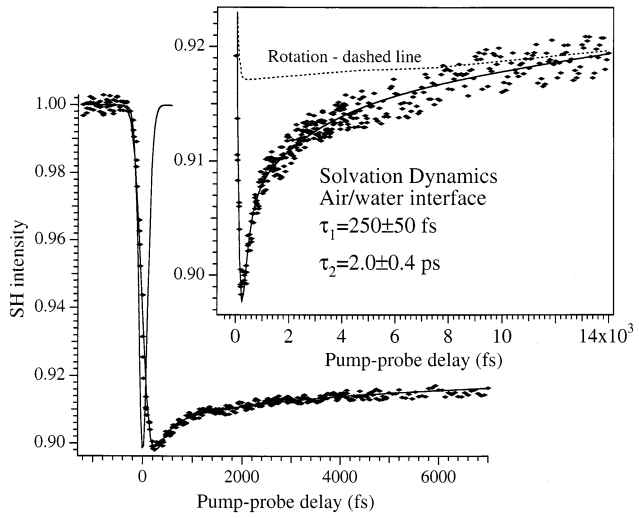

Figure 4. Pump−probe time-resolved second harmonic generation signal of C314 at the surfactant-free air/water interface. Inset: the ultrafast part of the response due to the solvation dynamics (note the change of both vertical and horizontal scales). Diamonds, experimental data; solid line, biexponential fit described in the text; dashed line, asymptote of the solvation dynamics (see text for details).

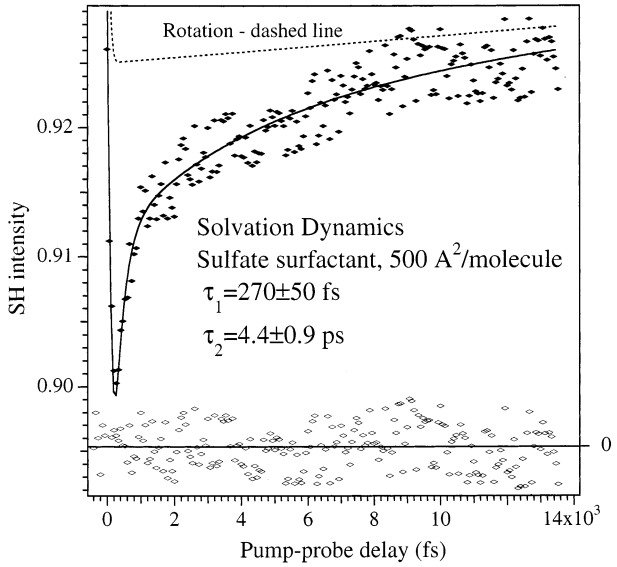

Figure 5. Solvation dynamics of C314 at the SDS $CH_3(CH_2)_{11}OSO_3^-$ air/water interface, 500 Å^2/SDS molecule (bulk concentration of SDS is 0.05 mM). Dashed line: rotational dynamics baseline (see text). Residual of the fit is shown at the bottom.

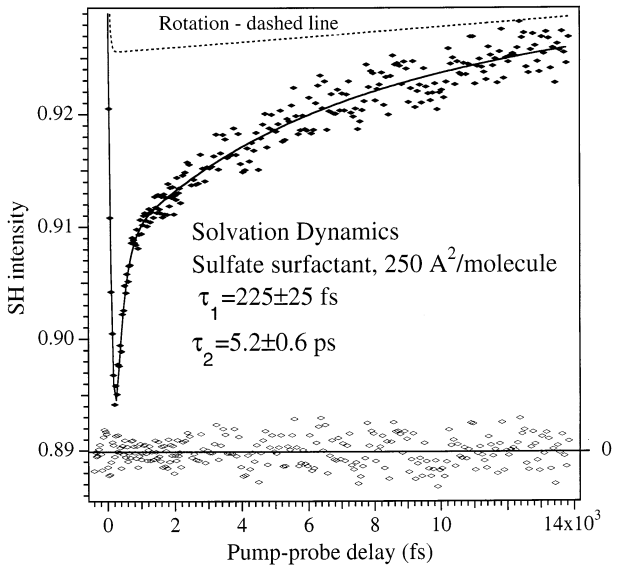

Figure 6. Solvation dynamics of C314 at the SDS air/water interface, 250 Å^2/SDS molecule (bulk concentration of SDS is 0.125 mM). Dashed line: rotational dynamics baseline (see text). Residual of the fit is shown at the bottom.

The main panel in Figure 4 shows the TRSHG signal (normalized to 1) recorded at the air/water interface; the partial recovery of the signal due to the solvation dynamics is detailed in the inset. The fitting procedure outlined below gives the solid line and allows extraction of the solvation correlation function $S(t)$.

The initial drop of the TRSHG signal is fitted as a convolution of a step-function with the instrument response function. The latter is determined as the pump−probe cross-correlation measured by the surface pump + probe sum frequency generation at the sample interface, and therefore represents the true experimental instrument response function. It is represented by a Gaussian with the full width at half-maximum $\tau_0 = 175$ fs. Absence of the coherent artifact in these experiments allows careful deconvolution of the instrument response from the transients. We do not detect the inertial solvation component, which is expected to be of the order of $\tau_i = 25$ fs and therefore is suppressed by a factor of τ_0/τ_i (almost 10) in the observed transient signal.

There are several components in the recovery of the TRSHG signal. In the 0−14 ps time window studied here, it is dominated by the solvation dynamics which clearly show a bimodal behavior. This solvation dynamics part is represented as a sum of two exponential functions with adjustable time constants τ_1 and τ_2 and amplitudes a_1 and a_2. Rotational relaxation of C314 proceeds on a much slower time scale[30] and provides a slightly sloping background for the solvation dynamics part of the TRSHG signal, ∼0.2% change per 10 ps. The rotational relaxation, which is a $t \rightarrow \infty$ asymptote for the solvation, was measured independently in a longer pump−probe delay scan for the chosen polarizations of the pump (*S*), probe (45°), and SH signal (*P*), and is shown by dashed line in Figures 4-7, where the amplitude of the bleach in the rotation dynamics signal has been scaled down for comparison purposes. It was found to be a single exponential with $\tau_R = 350$ ps, in good agreement with the previous report,[30] and was used in the fit with no adjustments. The overall recovery of the TRSHG signal is thus represented as a sum of three exponentials, with only two of them, representing the solvation part, having adjustable amplitudes and time constants.

The SH probe wavelength was chosen to be on the blue shoulder of the surface spectrum of C314 (420 nm, Figure 3) because our modeling shows that in this spectral range the recovery of the TRSHG signal $I_{SH}(t)$ gives a faithful representation of the solvation correlation function $S(t)$, that is, $I_{SH}(t)$ is approximately linearly proportional to $S(t)$.[18] For a model system with realistic spectral parameters, it was found that the direct fit of the TRSHG data reproduces the time scales of the dynamic Stokes shift $S(t)$ within 10−15%. Use of a single probe wavelength to extract the solvation dynamics correlation function is analogous to the so-called "linear probe wavelength" in the time-resolved fluorescence measurements in bulk liquids.[8,31] The fitting of the TRSHG signal as described above thus yields the solvation correlation function at the interface

$$S(t) = a_1 \exp(-t/\tau_1) + a_2 \exp(-t/\tau_2) \qquad (5)$$

The amplitudes a_1 and a_2 are normalized to one-half the magnitude of the initial bleach in the SH signal due to the pump,

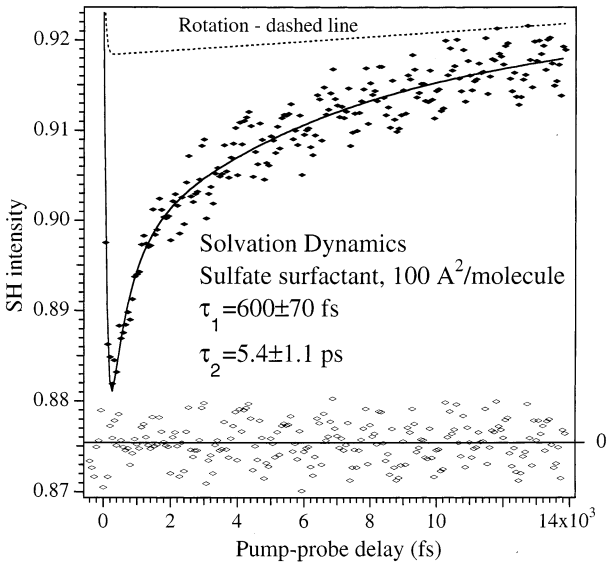

Figure 7. Solvation dynamics of C314 at the SDS air/water interface, 100 Å^2/SDS molecule (bulk concentration of SDS is 0.6 mM). Dashed line: rotational dynamics baseline (see text). Residual of the fit is shown at the bottom.

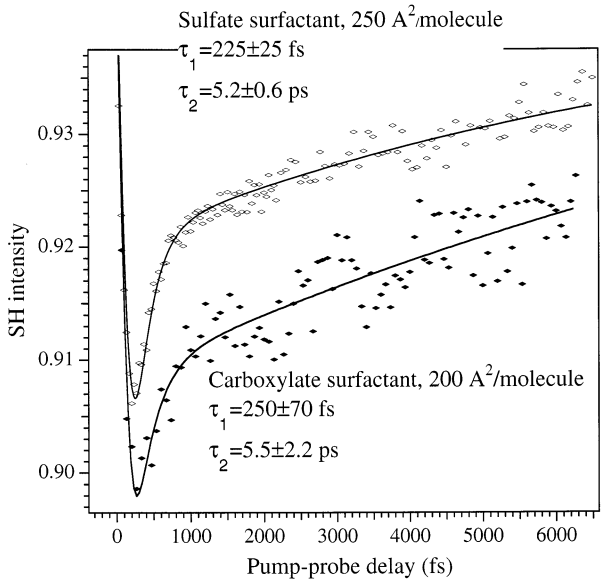

Figure 8. Comparison of the solvation dynamics of C314 at the air/water interface covered with SDS $CH_3(CH_2)_{11}OSO_3^-$, 250 Å^2/molecule (top trace), and ionized stearic acid $CH_3(CH_2)_{16}COO^-$, 200 Å^2/molecule (bottom trace).

i.e., ∼5% of the total SH signal. This is done for the following reason. The initial $t = 0$ bleach in the SH signal (∼10%) is due to the transfer of ∼5% of the population to the excited state, resulting in a 5% decrease of the ground-state contribution to the $\chi^{(2)}$ plus an opposite phase but same magnitude, i.e., −5%, contribution from the nascent excited-state population, as described by eq 4. Therefore, the initial decrease in SH signal would be 10%. If the solvation shifts the excited S_1 state far to the red, completely out of resonance with the SH probe, the SH signal would recover from 90 to 95% (the 5% "hole" in the ground-state population persists for a longer time determined by the orientational relaxation, vide supra). This would correspond to $a_1 + a_2 = 1$. In reality, $a_1 + a_2 < 1$ because by the completion of the solvation process there still is overlap of the excited-to-ground-state $S_1 \rightarrow S_0$ transition frequency $\omega_{eg}(t)$ with the SH probe.

Although the solvation dynamics of C314 at the neat air/water interface have been reported previously,[19] the improved signal-to-noise ratio in the present experiments allows unambiguous observation of the two diffusive solvation components, as demonstrated in Figure 4. The extracted time scales are $\tau_1 = 250 \pm 50$ fs ($a_1 = 0.5 \pm 0.12$) and $\tau_2 = 2.0 \pm 0.4$ ps ($a_2 = 0.24 \pm 0.08$). These results obtained using the 840 nm probe wavelength are in good agreement with the dynamics obtained using 900 nm probe in an earlier study, where the two components were also observed, $\tau_1 = 250 \pm 60$ fs and $\tau_2 = 1.2 \pm 0.4$ ps.[27] The amplitude-averaged solvation time $\langle\tau\rangle = (a_1\tau_1 + a_2\tau_2)/(a_1 + a_2)$ is 900 ± 150 fs, in agreement with the previously reported $\langle\tau\rangle = 820 \pm 60$ fs measured using the 840 nm probe.[27]

TRSHG signals of the C314 solvation dynamics recorded at the sodium dodecyl sulfate monolayers at the air/water interface are shown in Figures 5−7 for the three chosen surfactant concentrations, 500, 250, and 100 Å^2/SDS molecule. The biexponential character of the aqueous solvation response is evident at all three interfaces. Residuals of the fit, shown in empty diamonds at the bottom of Figures 5−7, demonstrate the noise level of 0.20, 0.13, and 0.23% for the three experiments, that is, the S/N ratio varies from 450 to 770. This proves critical in observation of the two solvation components because the dynamic range of the experiment, i.e., the change of the SH signal due to the excited state solvation, is only ∼3−4%.

For the 500 Å^2/SDS molecule interface, the faster solvation component is $\tau_1 = 270 \pm 50$ fs ($a_1 = 0.6 \pm 0.1$), i.e., essentially the same as at the surfactant-free air/water interface, whereas the slower component is elongated by more than a factor of 2, to $\tau_2 = 4.4 \pm 0.9$ ps ($a_2 = 0.22 \pm 0.04$). At the intermediate density monolayer, 250 Å^2/SDS molecule, the fast component is still unchanged with respect to the air/water interface, $\tau_1 = 225 \pm 25$ fs ($a_1 = 0.60 \pm 0.08$), and the slower component is longer yet, $\tau_2 = 5.2 \pm 0.6$ ps ($a_2 = 0.24 \pm 0.04$). Finally, at the highest SDS film density, 100 Å^2/SDS molecule, the faster component is elongated to $\tau_1 = 600 \pm 70$ fs ($a_1 = 0.40 \pm 0.04$), whereas the slower component is virtually the same as at the intermediate surfactant coverage, $\tau_2 = 5.4 \pm 1.1$ ps ($a_2 = 0.32 \pm 0.04$).

To determine whether the chemical composition of the negatively charged headgroup affects the dynamical properties of the aqueous interface, we compare the solvation dynamics at two different anionic surfactants, SDS and ionized stearic acid $CH_3(CH_2)_{16}COO^-$, at similar surfactant densities The recently reported measurements for the carboxylate monolayer[18] have been repeated to improve the signal-to-noise ratio. Figure 8 shows TRSHG signals at the 250 Å^2/SDS molecule monolayer (top trace) and 200 Å^2/molecule ionized stearic acid monolayer (bottom trace). For the carboxylate surfactant, the two solvation components are $\tau_1 = 250 \pm 70$ fs ($a_1 = 0.48 \pm 0.12$) and $\tau_2 = 5.5 \pm 2.2$ ps ($a_2 = 0.40 \pm 0.18$). The overall features of the solvation responses at the SDS and carboxylate interfaces are very similar; both the time scales τ_1 and τ_2 and their relative amplitudes a_1 and a_2 agree within the experimental error. The comparison suggests that the surface charge has a more significant effect on the solvation dynamics than the chemical structure of the amphiphile.

The results for the diffusive solvation dynamics components at various aqueous interfaces measured in the present study are summarized in Table 1, together with a compilation of the corresponding response times reported for bulk water.

TABLE 1: Diffusive Components of the Solvation Response Function at the Air/Water Interface, at Several Anionic Surfactant Densities, and in Bulk Water[a]

	τ_1	a_1	τ_2	a_2	$\langle\tau\rangle^b$
bulk water[a]	130−290 fs	0.7−0.3	0.69−1.2 ps	0.3−0.7	0.6−0.9 ps
surfactant-free air/water interface	250 ± 50 fs	0.5 ± 0.12	2.0 ± 0.4 ps	0.24 ± 0.08	0.9 ± 0.15 ps
SDS, 500 Å^2/molecule	270 ± 50 fs	0.6 ± 0.1	4.4 ± 0.9 ps	0.22 ± 0.04	1.4 ± 0.3 ps
SDS, 250 Å^2/molecule	225 ± 25 fs	0.6 ± 0.08	5.2 ± 0.6 ps	0.24 ± 0.04	1.65 ± 0.2 ps
ionized stearic acid, 200 Å^2/molecule	250 ± 70 fs	0.5 ± 0.12	5.5 ± 2.2 ps	0.4 ± 0.18	2.2 ± 0.9 ps
SDS, 100 Å^2/molecule	600 ± 70 fs	0.4 ± 0.04	5.4 ± 1.1 ps	0.32 ± 0.04	2.8 ± 0.4 ps

[a] A compilation of experimental results from refs 4, 5, 8, and 21. [b] The amplitude-averaged diffusive solvation time defined as $\langle\tau\rangle = (a_1\tau_1 + a_2\tau_2)/(a_1 + a_2)$.

Discussion

The solvation dynamics observed in our TRSHG experiments are most likely dominated by the dynamical response of the water solvent, which is faster, is more polar, and has a much higher number density at the interface than the lipid surfactant. We therefore begin by comparing our findings with the dynamics of the bulk water, for which it has been firmly established experimentally that the solvation response has three distinct temporal components.[5] The ultrafast inertial component, which accounts for ∼50% of the solvation free energy, is characterized by a 25 fs Gaussian decay. The other 50% of the solvation free energy is relaxed via two diffusive components which are exponential with time scales $\tau_1 = 130-290$ fs and $\tau_2 = 0.69-1.2$ ps (see Table 1). Theoretical models, including molecular dynamics simulations, assign the inertial component to the nearly free liberations of water molecules.[6,7] The diffusive solvation dynamics, on the other hand, are associated with the rotational and translational diffusional motions which are strongly coupled in water.[4,5,8] These motions cannot occur without breaking and making hydrogen bonds, i.e., involve rearrangement of the H-bond network. Indeed, time-resolved vibrational spectroscopy experiments in bulk water yielded average lifetimes of the OH···O hydrogen bond from 0.5 to 1 ps,[9,10] similar to the diffusive solvation time scales from the time-resolved fluorescence Stokes shift measurements of dipolar solutes. Inelastic neutron scattering experiments have been reported to yield the time scales for the rotational (1.16 ps) and translational (1.25 ps) self-diffusion in water.[32] The aqueous solvation dynamics are also closely connected with the intermolecular dynamics of neat water measured without a solvatochromic solute, using frequency- and time-resolved Raman scattering.[33]

Our measurements show that the diffusive aqueous solvation response is slower at negatively charged lipid interfaces than in bulk water. A qualitatively very similar trend has recently been reported for the H-bond dynamics of water in solvation shells of anions, measured using time-resolved vibrational spectroscopy.[22] The OH···O stochastic modulation time constant in hydration shells of F^-, Cl^-, Br^-, and I^- was measured to be from 0.8 to 3.0 ps, considerably slower than the 500 fs lifetime the OH stretch measured by the ultrafast vibrational spectroscopy in bulk water without the anions.[22] Thus, there is a semiquantitative agreement between the dynamics of hydrogen bonds in the hydration shells of anions in bulk water and the dynamics of solvation near the anionic headgroups of surfactants at the air/water interface. This agreement supports the close connection between the diffusive solvation response and the dynamical properties of the hydrogen bond network of water and, further, implies that this relation holds for interfacial aqueous systems as well as for the bulk water.

The existence of the two diffusive time scales τ_1 and τ_2 demonstrates the complexity of the aqueous solvation dynamics. Despite numerous theoretical efforts, at present there is no clear-cut assignment of the molecular motions of water contributing to the two diffusive components. Similar to the bulk water results, we observe two diffusive components at the air/water interface and at the anionic lipid interfaces. A significant finding is that the two time scales behave differently as a function of the surface charge. The faster τ_1 component is unaffected at low to intermediate surface charge densities (500 to 250 Å^2/SDS molecule) but increases by a factor of 3 at 100 Å^2/SDS molecule. On the contrary, the slower τ_2 component shows high sensitivity to the surface charge even at low surfactant densities, lengthening by more than a factor of 2 at 500 Å^2/SDS molecule, but changes little (∼20%) as the coverage is further increased to 100 Å^2/SDS molecule. To illustrate the difference between the two components, they are plotted in Figure 9 as a function of the SDS surface density.

Our measurements of the solvation dynamics at negatively charged interfaces, summarized in Figure 9, suggest that the two diffusive solvation components τ_1 and τ_2 involve substantially different motions of water. This difference may prove key to the assignment of these relaxation modes because it provides a test for theoretical modeling, such as MD simulations, of these aqueous interfaces.[34]

In Figure 9, the solvation dynamics time scales τ_1 and τ_2 are compared with the results of the static frequency domain vibrational SFG spectroscopy, which was recently used to study structure and orientation of water at the SDS air/water interface.[14,15] Two OH stretch bands have been observed at the interface. The higher frequency band (3300−3500 cm^{-1}), denoted OH−SS-A, has been assigned to the "water-like" structures with lower H-bond order, whereas the lower-frequency OH−SS−S band (3100−3300 cm^{-1}) was presumed to be due to "ice-like", high H-bond order structures specific to the interface.[35] Orientational alignment of water by the charged surface was manifested by an increase in the overall VSFG intensity. Increase of the relative intensity of the high H-bond order OH−SS−S band over the lower H-bond order OH−SS−A band with the surface charge density was interpreted as increased hydrogen bonding between water molecules at the negatively charged interface. In Figure 9, the VSFG electric field of the high H-bond order OH−SS−S band is shown by dashed line as a function of the charged surfactant density.

As can be seen in the bottom panel in Figure 9, the slower component τ_2 of the diffusive solvation response measured in our TRSHG experiments scales with the VSFG field of the strongly hydrogen-bonded OH stretch as the SDS surface density is increased. Although the trend is subject to relative large experimental uncertainties indicated by the error bars, it allows

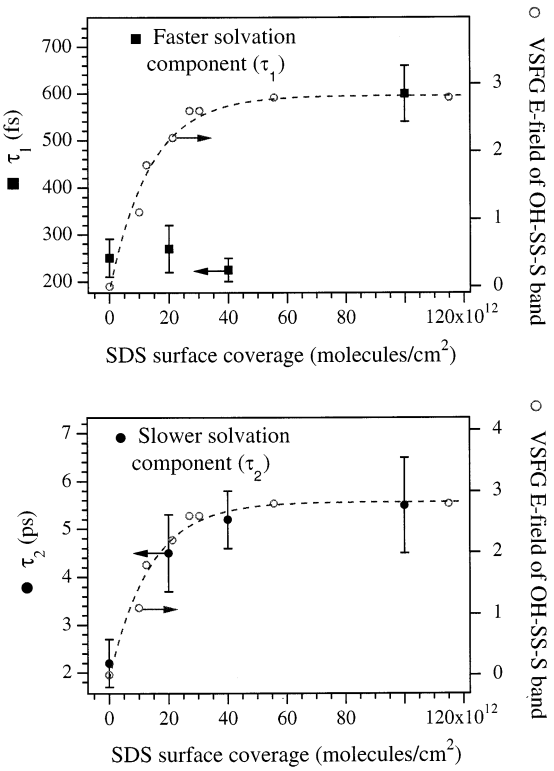

Figure 9. Dependence of the faster τ_1 (□, upper panel) and slower τ_2 (♦, lower panel) solvation dynamics time scales on the surface density of the anionic SDS surfactant. ○ (dashed line) shows comparison with the static alignment and increased hydrogen bonding of H_2O molecules at the negatively charged SDS interface, quantified as the VSFG electric field of the high H-bond order OH−SS−S stretch band measured by the SFG vibrational spectroscopy, refs 14 and 15 (see text).

us to infer that this slower relaxation mode is tied to the increased H bonding and alignment near the interface. That is, we may suggest that the slower τ_2 dynamical time scale of aqueous solvation at the interface corresponds to the strongly hydrogen bonded interfacial water structures characterized by the lower-frequency OH−SS−S band (3100−3300 cm^{-1}).

The upper panel of Figure 9 shows that the faster τ_1 component, on the contrary, exhibits different behavior as a function of the negative surface charge than the static VSFG measurement. We thus cannot connect this faster aqueous relaxation mode with spectral features of the OH stretch band measured at the interface by VSFG. The faster diffusive solvation component τ_1 has been reported by numerous both bulk-phase experiments, ranging from 130 to 250 fs,[4,5,8,21] as well as in our study at interfaces (Figures 4−8, Table 1). Nonetheless, the assignment of this faster aqueous solvation mode remains unknown. Its time scale appears somewhat faster than the typical H-bond dynamics time scales obtained from vibrational spectroscopy, of the order of 1 ps, yet significantly slower than the inertial librational response time of ∼25 fs. Molecular dynamics calculations, which would be based on the well developed methods for simulating liquid interfaces,[34] may help elucidate both the nature of the various vibrational OH bands at the interface and the origin of the two diffusive solvation dynamics time scales. This, however, is outside the scope of the present paper.

Solvation dynamics in the interior of reverse micelles have been reported, where the overall response is dominated by a much slower 0.1−0.3 ns time scale component (>60%) arising due to geometric restrictions.[21,36] However, examination of the faster part of the response (35−40%) shows that the τ_1 (subpicosecond) and τ_2 (picosecond) components are lengthened compared with the solvation dynamics in bulk water and at the air/water interface. On the basis of our observations at the planar charged lipid interfaces, this can be attributed to the effect of the surface charge of the reverse micelles.

Ultrafast solvation response was recently measured in the aqueous hydration shells of a protein (histone I) and protein−DNA complex by using an anionic probe dye molecule which noncovalently binds to the positively charged residues of the protein.[20] It was found that, unlike the case of micelles, the solvation in the protein water layer is not hindered geometrically and still occurs on fs to ps time scale, although somewhat slower than in bulk water. This is consistent with the interfacial electric field effect observed in our measurements, which caused the overall slower aqueous solvation dynamics at charged lipid monolayers. We note, however, that significant differences may exist between the negatively and positively charged interfaces. Polar alignment of water molecules at oppositely charged interfaces, i.e., hydrogen pointing up at negative surfaces vs oxygen up at positive surfaces, has been observed by SFG[14] and X-ray scattering.[16] This necessarily implies that different H-bonding structures are present at the negatively and positively charged interfaces, which may result in different dynamics. We are planning TRSHG experiments at aqueous interfaces of positively charged lipid surfactants to elucidate the effect of the sign of the interfacial charge on the solvation process.

Conclusions

The diffusive part of the aqueous solvation dynamics was measured at anionic lipid interfaces using the surface-specific, ultrafast time-resolved second harmonic generation (TRSHG) technique. The diffusive solvation, which is associated with rearrangement of the hydrogen bond network of water, was found to be biexponential at the anionic surfactant interfaces. In agreement with previous reports[27] and theoretical models,[34] solvation at the surfactant-free air/water interface was found to be similar to the bulk water response. The overall effect of the negatively charged lipid monolayer with a surface charge density comparable to that of a typical biointerface (100 Å^2/molecule) is to slow the diffusive solvation response by a factor of ∼3−5 compared to the bulk water. This is consistent with the increased H-bond order observed at the charged water interfaces using equilibrium structure-sensitive techniques such as vibrational sum-frequency generation spectroscopy.[14,15]

More detailed information about the molecular nature of the diffusive aqueous solvation is available from measurements of the two diffusive solvation time scales at different anionic surfactant coverages. The two time scales exhibit different behavior as a function of the surface charge density, which demonstrates that they are associated with significantly different molecular motions of water. Comparison of our time-resolved dynamical experiments with the structure-sensitive vibrational spectroscopy measurements by others[14,15] allows connections to be made between the dynamical properties of the water solvent at the interface and its equilibrium structure. For the first time, to our knowledge, the dynamical time scale of a diffusive solvation component in water is related to a spectral feature of the vibrational spectrum that characterizes strongly H-bonded equilibrium water structures at the charged interface.

Nearly identical solvation responses have been recorded at the carboxylate ($CH_3(CH_2)_{16}COO^-$) and sulfate ($CH_3(CH_2)_{11}OSO_3^-$) anionic surfactant interfaces, suggesting that for these anionic lipids the solvation dynamics are sensitive to the electrical charge of the interface rather than the chemical composition of the hydrophilic headgroup.

Both equilibrium and dynamical properties of water as a solvent are affected by the negatively charged lipid interface, although the solvation dynamics proved to be more sensitive to the molecular properties, structure, and interactions at the interface than the static measurements of equilibrium solvation energies, i.e., interfacial polarity. The changed behavior of the hydrogen bond network near anionic interfaces may have profound effect on many interfacial processes, affecting adsorption equilibria, solvation energies, chemical equilibria and rates of reactions such as electron transfer, hydrogen bonding, and molecular friction.

Acknowledgment. This research was supported by grants from the National Science Foundation and from the Division of Chemical Science, Office of Basic Energy Sciences, of the Department of Energy. The authors also acknowledge Mr. Joel Henzie for his contributions to this research project.

References and Notes

(1) Eisenthal, K. B. *Acc. Chem. Res*. **1993**, *26*, 636; *J. Phys. Chem*. **1996**, *100*, 12997.
(2) Marcus, R. A. *J. Chem. Phys*. **1956**, *24*, 966.
(3) Heitele, H. *Angew. Chem., Int. Ed. Engl*. **1993**, *32*, 359.
(4) Maroncelli, M. *J. Mol. Liquids* **1993**, *57*, 1.
(5) Jimenez, R.; Fleming, G. R.; Kumar, P. V.; Maroncelli, M. *Nature* **1994**, *369*, 471.
(6) Maroncelli, M.; Kumar, P. V.; Papazyan, A. *J. Phys. Chem*. **1993**, *97*, 13.
(7) Maroncelli, M.; Fleming, G. R. *J. Chem. Phys*. **1988**, *89*, 5044.
(8) Barbara, P. F.; Jarzeba, W. *Adv. Photochem*. **1990**, *15*, 1.
(9) Laenen, R.; Rauscher, C.; Laubereau, A. *Phys. Rev. Lett*. **1998**, *80*, 2622.
(10) Woutersen, S.; Emmerichs, U.; Nienhuys, H.-K.; Bakker, H. J. *Phys. Rev. Lett*. **1998**, *81*, 1106.
(11) Gennis, R. B. *Biomembranes, Molecular Structure and Function*; Springer-Verlag: New York, 1989.
(12) Habib, M. A.; Bockris, J. O'M. *Langmuir* **1986**, *2*, 388.
(13) Ataka, K.; Yotsuyanagi, T.; Osawa, M. *J. Phys. Chem*. **1996**, *100*, 10664.
(14) Gragson, D. E.; McCarty, B. M.; Richmond, G. L. *J. Am. Chem. Soc*. **1997**, *119*, 6144.
(15) Gragson, D. E.; Richmond, G. L. *J. Am. Chem. Soc*. **1998**, *120*, 366.
(16) Toney, M. F.; Howard, J. N.; Richer, J.; Borges, G. L.; Gordon, J. G.; Melroy, O. R.; Wiesler, D. G.; Yee, D.; Sorensen, L. B. *Nature* **1994**, *368*, 444. Gordon, J. G.; Melroy, O. R.; Toney, M. F. *Electrochim. Acta* **1995**, *40*, 3.
(17) Benderskii, A. V.; Eisenthal, K. B. *J. Phys. Chem. B* **2000**, *104*, 11723.
(18) Benderskii, A. V.; Eisenthal, K. B. *J. Phys. Chem. B* **2001**, *105*, 6698.
(19) Zimdars, D.; Dadap, J. I.; Eisenthal, K. B.; Heinz, T. F. *Chem. Phys. Lett*. **1999**, *301*, 112.
(20) Zhong, D.; Pal, S. K.; Zewail, A. H. *Chem. Phys. Chem*. **2001**, *2*, 219.
(21) Pant, D.; Riter, R. E.; Levinger, N. E. *J. Chem. Phys*. **1998**, *109*, 9995. Riter, R. E.; Undiks, E. P.; Levinger, N. E. *J. Am. Chem. Soc*. **1998**, *120*, 6062. Riter, R. E.; Willard, D. M.; Levinger, N. E. *J. Phys. Chem. B* **1998**, *102*, 2705.
(22) Kropman, M. F.; Bakker, H. J. *Science* **2001**, *291*, 2118.
(23) Chattoraj, D. K.; Birdi, K. S. *Adsorption and the Gibbs Surface Excess*, Plenum Press: New York, 1984.
(24) Zhao, X.; Goh, M. C.; Eisenthal, K. B. *J. Phys. Chem*. **1990**, *94*, 2222. Zhao, X.; Goh, M. C.; Subrahmanyan, S.; Eisenthal, K. B. *J. Phys. Chem*. **1990**, *94*, 3370.
(25) Heinz, T. F.; Tom, H. W. K.; Shen, Y. R. *Phys. Rev. A* **1983**, *28*, 1883.
(26) Moylan, C. R. *J. Phys. Chem*. **1994**, *98*, 13513.
(27) Zimdars, D.; Eisenthal, K. B. *J. Phys. Chem. B* **2001**, in press.
(28) Wang, H.; Borguet, E.; Eisenthal, K. B. *J. Phys. Chem. A* **1997**, *101*, 713; *J. Phys. Chem. B* **1998**, *102*, 4927.
(29) Shen, Y. R. *The Principles of Nonlinear Optics*; Wiley-Interscience: New York, 1984.
(30) Zimdars, D.; Dadap, J. I.; Eisenthal, K. B.; Heinz, T. F. *J. Phys. Chem. B* **1999**, *103*, 3425.
(31) Gardecki, J. A.; Maroncelli, M. *J. Phys. Chem. A* **1999**, *103*, 1187.
(32) Teixeira, J.; Bellissent-Funel, M.-C.; Chen, S. H.; Dianoux, A. J. *Phys. Rev. A* **1985**, *31*, 1913.
(33) Castner, E. W.; Chang, Y. J.; Chu, Y. C.; Walrafen, G. E. *J. Chem. Phys*. **1995**, *102*, 653.
(34) Benjamin, I. *Chem. Rev*. **1996**, *96*, 1449.
(35) Du, Q.; Freysz, E.; Shen, Y. R. *Science* **1994**, *72*, 238.
(36) Faeder, J.; Ladanyi, B. M. *J. Phys. Chem. B* **2000**, *104*, 1033.